Materials Transactions, Vol. 54, No. 3 (2013) pp. 291 to 296

Magnetoresistance and Transformation Hysteresis in the $Ni_{50}Mn_{34.4}In_{15.6}$ Metamagnetic Shape Memory Alloy

Rie Y. Umetsu[1,*], Keita Endo[2,3], Akihiro Kondo[4], Koichi Kindo[4], Wataru Ito[5], Xiao Xu[3], Takeshi Kanomata[2,3] and Ryosuke Kainuma[3]

[1]*Institute for Materials Research, Tohoku University, Sendai 980-8577, Japan*
[2]*Faculty of Engineering, Tohoku Gakuin University, Tagajo 985-8537, Japan*
[3]*Department of Materials Science, Graduate School of Engineering, Tohoku University, Sendai 980-8579, Japan*
[4]*Institute for Solid State Physics, The University of Tokyo, Kashiwa 277-8581, Japan*
[5]*Department of Materials and Environmental Engineering, Sendai National College of Technology, Natori 981-1239, Japan*

Temperature dependence of the equilibrium transformation field (H_0) for $Ni_{50}Mn_{34.4}In_{15.6}$ metamagnetic shape memory alloy was precisely determined by electrical resistivity measurements using a pulsed magnet. The H_0-T curve was found to exhibit a maximum at around 50 K, suggesting that the transformation entropy change becomes negative in the lower temperature region. The residual electrical resistivity in the field-induced parent phase at lower temperatures was about $10 \times 10^{-8}\,\Omega\cdot m$, being normal value as the ferromagnetic alloys, whereas that in the martensite phase was high of about $200 \times 10^{-8}\,\Omega\cdot m$. The temperature dependence of the magnetic field hysteresis can be well fitted with the Seeger's theory proposed for plastic deformation by dislocations. [doi:10.2320/matertrans.M2012365]

(Received November 2, 2012; Accepted December 20, 2012; Published February 16, 2013)

Keywords: *nickel-based Heusler alloys, metamagnetic shape memory alloy, magnetic field-induced reverse transformation, magnetoresistance effect*

1. Introduction

Since the report of a large magnetic field-induced strain for Ni_2MnGa single-crystalline alloy,[1)] ferromagnetic shape memory alloys (FSMAs) have received much attention as high performance actuator materials. An unusual type of FSMAs in the Ni–Mn–Z (Z = In, Sn and Sb) Heusler alloys and their Co-doped alloys have been found.[2–7)] In these alloys, the martensitic transformation starting temperature, T_{Ms}, and the reverse transformation finishing temperature, T_{Af}, drastically decrease by application of a magnetic field, and a magnetic field-induced transformation, namely, a kind of metamagnetic phase transformation, has been confirmed in the martensite (M) phase. Accompanying this martensitic transformation, large magnetoresistance so-called metamagnetic shape memory effect,[8–11)] magnetic superelasticity[12)] and large inverse magnetocaloric effects,[12–15)] and drastic change of the thermal transport properties[16–18)] have also been reported. The decrease of the martensitic transformation temperatures are originated from the effect that the free energy of the ferromagnetic parent (P) phase becomes lower by applied magnetic field.

Our group has recently reported that the martensitic transformation in the quaternary Ni–Co–Mn–In alloy is interrupted at a specific temperature, T_A, during field cooling and does not further proceed.[19)] From the temperature dependence of the equilibrium transformation field assumed as $H_0 = (H_{Af} + H_{Ms})/2$, it was confirmed that the dH_0/dT becomes almost zero in the temperature region below the T_A, where H_{Af} and H_{Ms} are the reverse transformation finishing magnetic field and the forward transformation starting magnetic field, respectively. This behavior can be phenomenologically be explained by thermodynamic consideration using the Clausius-Clapeyron relation.[19)]

In the case of the ternary Ni–Mn–In system, Sharma *et al.*[20)] have pointed out that in the $Ni_{50}Mn_{34}In_{16}$ alloy, the martensitic transformation is kinetically arrested in a high magnetic field, as observed in $Ce(Fe,Al)_2$ and $(La,Pr,Ca)MnO_3$ exhibiting a first-order phase transformation from antiferromagnetism to ferromagnetism.[21,22)] We have also observed the thermal transformation arrest (which was called "kinetic arrest" in our previous papers) phenomenon in the $Ni_{50}Mn_{34}In_{16}$ alloy and reported a further abnormal behavior in the H_0-T curve, where the sign of $-dH_0/dT$ clearly becomes negative in the temperature region below T_A of about 80 K.[23,24)] Magnetic measurements in a wide magnetic field range up to 30 T using a pulsed magnet were also performed to investigate the spontaneous magnetization of the field-induced P phase for $Ni_{50}Mn_{34.4}In_{15.6}$ and $Ni_{50}Mn_{36}In_{14}$ alloys.[25)] Although the H_0-T curves in the Ni–Mn–In alloys have roughly been determined by not only the magnetization measurement, but also electrical resistivity measurement,[8–11)] more detailed investigations are required for further discussion of this unique phenomenon.

Recently, novel alloys with near-zero thermal hysteresis have been reported in quaternary Ti–Ni–Cu–Pd shape memory alloys.[26)] According to Cui *et al.*, there are two conditions obtaining the extremely small hysteresis. The first is no volume change due to the martensitic transformation and the second is an eigenvalue: $\lambda_2 = 1$.[27)] In contrast to this, there have been very few investigations for the temperature dependence of the hysteresis in low temperature region, such as a liquid helium temperature. The FSMAs are suitable to examine the temperature dependence of the hysteresis, because the magnetic field-induced martensitic transformation can be obtained in wide temperature range when magnetic measurement for appropriate specimens is performed in a wide magnetic field range. In the present study, the magnetoresistance measurements were systematically carried out for the $Ni_{50}Mn_{34.4}In_{15.6}$ in temperature

*Corresponding author, E-mail: rieume@imr.tohoku.ac.jp

range from 4.2 to 260 K and under magnetic fields up to 40 T with a pulsed magnet. The magnetic field hysteresis of the presented metamagnetic shape memory alloy was examined and the behavior of its temperature dependence was discussed.

2. Experimental Procedures

A polycrystalline specimen of the $Ni_{50}Mn_{34.4}In_{15.6}$ (at%) alloy was prepared by arc melting under an argon gas atmosphere of appropriate quantities of the constituent elements, namely, 99.99% pure Ni, 99.95% pure Mn and 99.99% pure In. The ingot was annealed at 1123 K for 3 days in a vacuum and then quenched in water. The crystal structure at room temperature was confirmed by X-ray powder diffraction as the $L2_1$-type structure and the lattice parameter was found to be 0.6004 nm. Magnetic measurements were performed using a superconducting quantum interference device magnetometer, and the electrical resistivity as a function of the magnetic field was measured by the conventional four probes method with a pulsed magnet up to 40 T installed in the Institute for Solid State Physics, The University of Tokyo, the width of the single-pulsed magnetic field being about 35 ms.

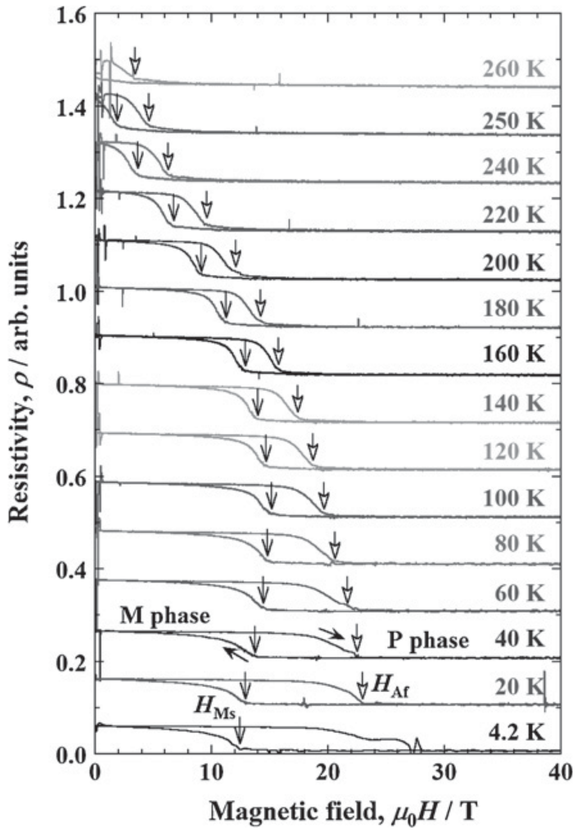

Fig. 1 Electrical resistivity as a function of the magnetic field with a pulsed magnet up to 40 T measured at several temperatures for the $Ni_{50}Mn_{34.4}In_{15.6}$ alloy.

3. Experimental Results and Discussions

3.1 Magnetoresistance and thermodynamic consideration

Electrical resistivity vs. magnetic field (ρ-H) curves obtained by the pulsed magnetic field up to 40 T at various temperatures in the $Ni_{50}Mn_{34.4}In_{15.6}$ alloy are shown in Fig. 1, where H_{Af} and H_{Ms} indicated by arrows are the reverse transformation finishing magnetic field and the martensitic transformation starting magnetic field during increase and decrease of the magnetic field, respectively. The magnetoresistance effects associated with the magnetic field-induced transformation are clearly observed. In all the obtained curves except the 4.2 and 260 K curves, the H_{Af} and H_{Ms} in the increase and decrease processes of the magnetic field, respectively, can easily be defined as indicated by the arrows. It is clearly seen that while both the H_{Af} and H_{Ms} increase with decreasing temperature, the H_{Ms} starts to decrease from 100 K, and that the field hysteresis gradually increases from about 140 K. Details of the behavior of H_{Af} and H_{Ms} as a function of the applying magnetic fields will be discussed later.

The electrical resistivity vs. temperature (ρ-T) curve in zero magnetic field and the thermomagntization (M-T) curve in a magnetic field of 0.1 T[25] for the $Ni_{50}Mn_{34.4}In_{15.6}$ alloy are shown in Fig. 2, together with ρ and M of the field-induced parent phase obtained at 40 T in the Fig. 1 and Ref. 25). Drastic changes of the electrical resistivity and the magnetization associated to the martensitic transformation are clearly confirmed at around 250 K. From the measurements, the martensitic transformation starting temperature, T_{Ms}, the reverse transformation finishing temperature, T_{Af}, and the Curie temperature, T_C, are evaluated to be 264, 254 and 306 K, respectively. As shown in Fig. 2(a), the ρ in the P phase gradually decreases with decreasing temperature, and the residual electrical resistivity is about $10 \times 10^{-8}\,\Omega{\cdot}m$, comparable to those in the normal ferromagnetic alloys, whereas the residual electrical resistivity in the M phase is high of about $200 \times 10^{-8}\,\Omega{\cdot}m$. The origin of the high value in residual resistivity of the M phase is unclear, although the large magnetoresistance behavior, which originates such a drastic change of the electrical resistivity due to the reverse martensitic transformation, is very beneficial to the applications. On the other hand, as shown by the M-T curves of Fig. 2(b), the M in the M phase is significantly lower than that in the P phase and in the lower temperature region, a slight magnetic cooling effect, i.e., the irreversibility between the zero-field-cooled (ZFC) and field-cooled (FC) M-T curves, is observed. In our resent study on the AC susceptibility measurements for $Ni_{50}Mn_{35}In_{15}$ alloy, the magnetic feature of the ground state is concluded to be magnetic blocking because of the existence of this magnetic cooling effect and frequency dependence of the AC susceptibility, in addition, the absent of the negative divergence of the non-linear part in the AC susceptibility.[28] The ground state of the present alloy would be similar to that of the $Ni_{50}Mn_{35}In_{15}$ alloy.

The differences in electrical resistivity, $\Delta\rho$, between the M phase and the P phase estimated at several temperatures in Fig. 2(a) are plotted in Fig. 3, together with those in magnetization, ΔM, extracted from the experimental data reported in Ref. 25), where the $\Delta\rho$ and the ΔM are indicated in the ρ-T and M-T curves of Figs. 2(a) and 2(b), respectively. The ΔM is given as the difference between M at 40 T and at 0.1 T in the FC process. It is seen that both $\Delta\rho$ and ΔM are

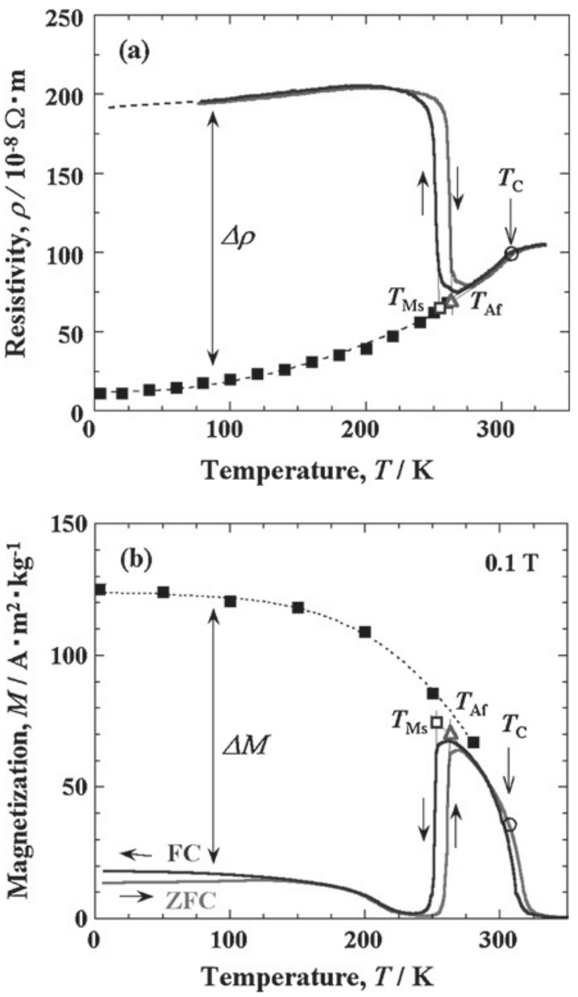

Fig. 2 (a) Temperature dependence of the electrical resistivity, ρ, in zero magnetic field and (b) the magnetization, M, measured in a magnetic field of 0.1 T, together with ρ and M of the field-induced parent phase obtained at 40 T in the Fig. 1 and Ref. 25). T_{Ms} (□), T_{Af} (△) and T_C (○) mean the martensitic transformation starting temperature, the reverse transformation finishing temperature and the Curie temperature, respectively.

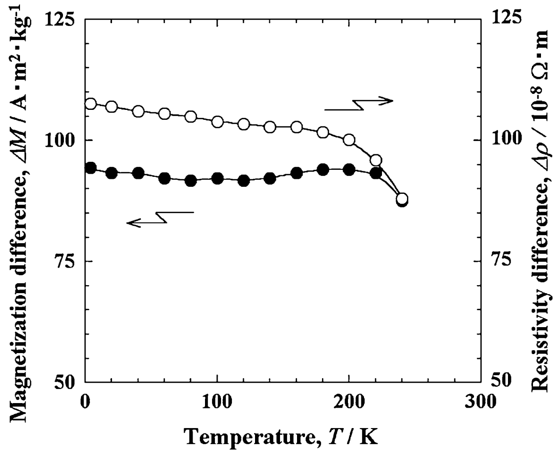

Fig. 3 Temperature dependence of difference of the magnetization, ΔM, and of the electrical resistivity, $\Delta\rho$, between the martensite phase and the parent phase. Here, ΔM is given as the difference between M at 40 T and at 0.1 T in the field-cooled (FC) process.

almost constant at temperatures below 200 K and that their temperature dependences are very similar to each other. Such a similarity suggests the existence of some relationship between the ρ and the M in the transformation.

Figure 4(a) indicates the temperature dependence of H_{Af}, H_{Ms} and H_0 obtained from the ρ-H curves in Fig. 1. Here, equilibrium magnetic field, H_0, is assumed as $H_0 = (H_{Ms} + H_{Af})/2$. The H_0-T curve basically accords with our previous report by magnetization measurements with a pulsed magnet as indicated by open symbols.[25] The H_0 starts to increase from the T_{Ms} of about 260 K with decreasing temperature, exhibits a maximum at around 50 K and then slightly decreases. According to the Clausius-Clapeyron relation in the magnetic phase diagram, the slope of the H_0-T curve, i.e., $\mathrm{d}H_0/\mathrm{d}T$, is given by

$$\mathrm{d}H_0/\mathrm{d}T = -\Delta S/\Delta M, \quad (1)$$

where the ΔS is the transformation entropy change. From eq. (1), the ΔS can be evaluated by

$$\Delta S = -\Delta M \cdot \mathrm{d}H_0/\mathrm{d}T. \quad (2)$$

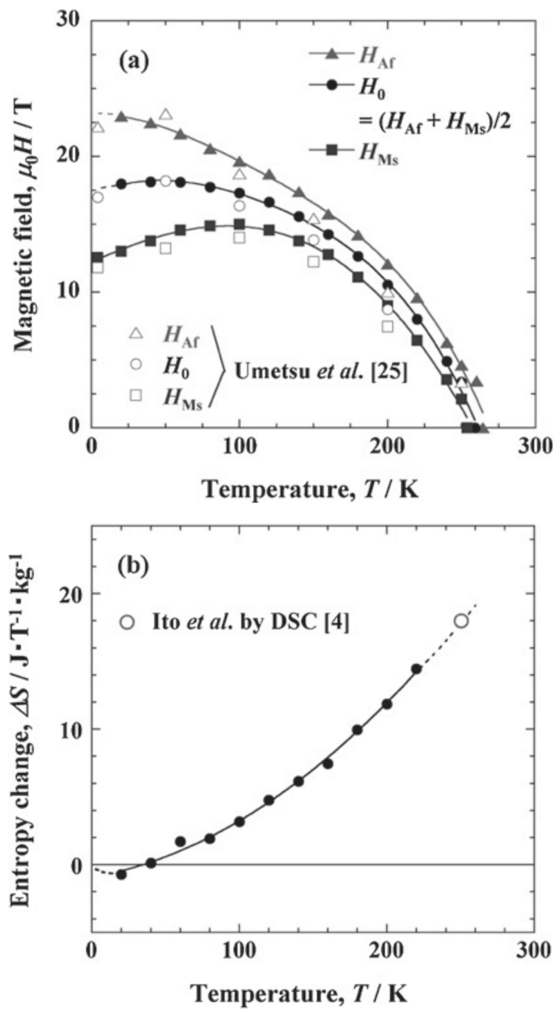

Fig. 4 (a) Temperature dependence of the equilibrium magnetic field H_0 obtained from the ρ-H curves, where H_0 is assumed as $H_0 = (H_{Ms} + H_{Af})/2$, H_{Ms} and H_{Af} are the magnetic fields in which the reverse transformation finishes and the martensitic transformation starts during the increase and decrease of the magnetic field, respectively. Open symbols are obtained by magnetization measurements.[25] (b) Temperature dependence of the entropy change, ΔS ($= -\Delta M \cdot \mathrm{d}H_0/\mathrm{d}T$); here, $\mathrm{d}H_0/\mathrm{d}T$ is obtained by the H_0-T curves in (a), and by ΔM in Fig. 3, together with reported value obtained by the DSC measurement.[4]

Figure 4(b) shows the ΔS obtained by eq. (2) with the combination of experimental values of the dH_0/dT in Fig. 4(a) and the ΔM in Fig. 3. When we discussed the temperature dependence of the ΔS in previous reports,[24] the values of ΔM were assumed to be constant. Since the ΔM and $\Delta\rho$ are actually not so sensitive to the temperature as shown in Fig. 3, the ΔS values evaluated with a constant ΔM in the previous paper seem to be not so far from the precise data. As indicated in the Fig. 4(b), the ΔS basically increases with increasing temperature and reaches the value determined by differential scanning calorimetric measurement at about 250 K.[4] In the low temperature region, becoming zero at around 40 K, the ΔS is negative at temperatures below 40 K. The negative ΔS means that the thermodynamic relative stability of the P phase to the M phase increases with cooling. Such an unusual behavior of the ΔS may be caused by an additional contribution of the magnetic term in the Gibbs free energy for the P phase, and has also been pointed out in a previous report for the $Ni_{50}Mn_{34}In_{16}$ alloy.[24] The driving force of the martensitic transformation, ΔG, is given by $\Delta G = \Delta T_{sp} \cdot \Delta S$, with the supercooling temperature for the transformation ΔT_{sp}. Therefore, the temperature (about 40 K), at which the ΔS becomes almost zero, is expected to coincide with the temperature, where the thermal transformation arrests below T_A. The T_A depends on the composition and alloy system, for example, T_A for $Ni_{45}Co_5Mn_{36.7}In_{13.3}$, $Ni_{50}Mn_{34}In_{16}$, $Ni_{44.4}Co_{5.1}Mn_{30.5}Al_{20.2}$ and $Ni_{33}Co_{13.4}Mn_{39.7}Ga_{13.9}$ are about 140, 80, 40 and 120 K, respectively.[19,24,29,30] Further systematic studies are required in order to clarify what factor mainly plays a role in the value of the T_A.

3.2 Transformation hysteresis

The hysteresis in martensitic transformation is known to be mainly caused by the friction in habit plane motion. If the thermodynamic equilibrium condition between the P phase and the M phase is approximately given at the center position in hysteresis, half of the hysteresis corresponds to "supercooling" field in order to overcome the friction. In the case of magnetic field-induced transformation, the field to overcome the friction is half of the magnetic hysteresis, $H_{hys}/2$, where $H_{hys} = H_{Af} - H_{Ms}$. Figure 5 shows the $H_{hys}/2$ obtained at each temperature examined in the present study. It is seen that while being almost constant at about 1.4 T in the temperature region above 200 K, the $H_{hys}/2$ gradually starts to increase with decreasing temperature at around 200 K and seems to reach about 7 T at 0 K. This temperature dependence is very similar to that of the apparent shear stress, τ_{app}, proposed by the Seeger's theory for spontaneous plastic deformation in the alloys with dislocation-obstacle interaction.[31–34]

According to Kocks *et al.*, Mecking and Kocks, and Ghosh and Olson,[35–37] the τ_{app} is given by a sum of two components: the thermal component, τ_{th}, which is necessary to overcome some activation energy Q, and the athermal resisting stress, τ_μ, unaffected by thermal activation process, i.e.,

$$\tau_{app}(T) = \tau_\mu + \tau_{th}(T), \tag{3}$$

and the stress dependence of activation energy Q for a rigid barrier with an average height Q_{0K} at 0 K is generally given as such a power law;

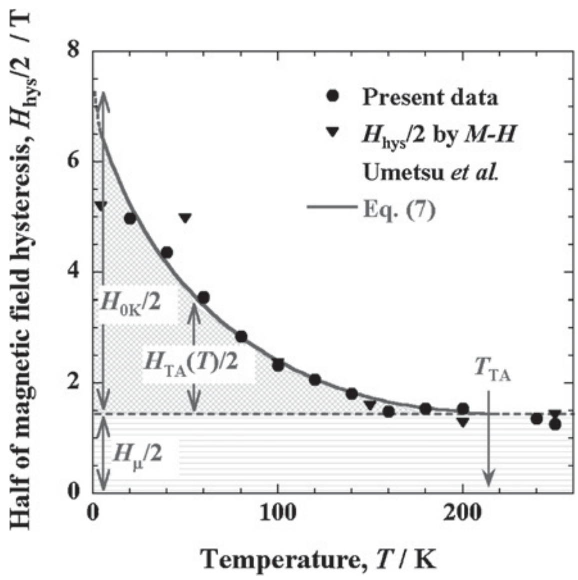

Fig. 5 Temperature dependence of half of the magnetic field hysteresis, $H_{hys}/2$, obtained from the ρ-H curves, together with that obtained by magnetization measurements;[25] here, H_{hys} is given as $H_{hys} = (H_{Af} - H_{Ms})$. The $H_{hys}/2$ are divided into the athermal and thermal components, $H_\mu/2$ and $H_{TA}(T)/2$. Solid line is drawn by eq. (7) with $p = 1/2$ and $q = 3/2$. T_{TA} is the temperature where $H_{TA}(T)/2$ becomes zero.

$$Q(\tau_{th}, T) = Q_{0K}(T)\left[1 - \left(\frac{\tau_{th}}{\tau_{0K}}\right)^p\right]^q. \tag{4}$$

Here, T is temperature and τ_{0K} the critical resolved shear stress at $T = 0$ K. The exponents, p and q are fitting parameters for the dislocation-obstacle interaction profile, and generally $0 \le p \le 1$ and $1 \le q \le 2$, which depend on the mechanism of the dislocation-obstacle interaction.[35] Since the Q is provided by the thermal vibration of atoms, which has a linear relation to temperature,

$$Q = mk_BT, \quad \text{and} \quad m = \ln(\dot{\gamma}_0/\dot{\gamma}) \tag{5}$$

where, m and k_B are the constant and the Boltzmann constant, respectively. $\dot{\gamma}$ is the shear rate and $\dot{\gamma}_0$ is the pre-exponential factor in the Boltzmann distribution friction. Here, m and $\dot{\gamma}$ have positive values and there is a relation $0 < \dot{\gamma} < \dot{\gamma}_0$. From eqs. (3)–(5), the apparent shear stress is given by

$$\tau_{app}(T) = \tau_\mu + \tau_{0K}\left[1 - \left(\frac{mk_BT}{Q_{0K}}\right)^{1/q}\right]^{1/p}. \tag{6}$$

If the habit plane motion during the magnetic field-induced transformation observed in the present study is equivalent to this shear deformation, since the ΔM is almost constant to temperature as shown in Fig. 2, eq. (6) can be modified with magnetic-field instead of the stress-field as follows:

$$\begin{aligned}\frac{1}{2}H_{hys}(T) &= \frac{1}{2}H_\mu + \frac{1}{2}H_{TA}(T)\\ &= \frac{1}{2}H_\mu + \frac{1}{2}H_{0K}\left[1 - \left(\frac{mk_BT}{Q_{0K}}\right)^{1/q}\right]^{1/p},\end{aligned} \tag{7}$$

where, H_μ and $H_{TA}(T)$ are the athermal and thermal components, respectively, in the "supercooling" magnetic-field to drive the habit plane against the friction, and H_{0K} is the value of $H_{TA}(T)$ at 0 K. As shown in Fig. 5, the $H_\mu/2$ and the $H_{0K}/2$ are estimated from a fitting by eq. (7) as being about 1.4 and 5.9 T, respectively, and a fitting curve in good agreement with the experimental plots is obtained with the combination of $p = 1/2$ and $q = 3/2$. Here, T_{TA} is the temperature, where $H_{TA}(T)/2$ becomes zero, that is, the temperature where the magnetic field-induced transformation is perfectly activated without any assistance of external field, and T_{TA} is about 214 K. In this phenomenological description, the combination of the p and q in eq. (7) is related to the shape of the dislocation-obstacle interaction profile and governs the shape of the H_{hys}-T profile. The combination of the values of p and q in plastic deformation is theoretically predicted, depending on the different types of interaction mechanisms between dislocations and some obstacles, such as the strain field of solute atoms, the generation of the anti-phase boundary and the obstacles with an elastic constant different from that in the matrix etc.[35] The combination of $p = 1/2$ and $q = 3/2$ used in the fitting curve of Fig. 5 is generally given for the interaction between dislocations and the strain field of solute atoms in the case of plastic deformation. Although the meaning of the combination of p and q in the present case is unclear, the Seeger's phenomenological theory is useful to describe the behavior of transformation hysteresis in the martensitic transformation. It is known from eq. (7) that the magnetic hysteresis, that is one of the most important factors in its practical use, depend on not only temperature, but also on the application rate of the magnetic field, and that the maximum hysteresis is given by $H_{hys} = H_\mu + H_{0K}$ at $\dot{\gamma} = \dot{\gamma}_0$, independent of temperature. Further study for a deeper understanding of the obtained results is required.

4. Conclusions

The equilibrium transformation field (H_0) as a function of the temperature for $Ni_{50}Mn_{34.4}In_{15.6}$ metamagnetic shape memory alloy was established by electrical resistivity measurements with using a pulsed magnet up to 40 T. A magnetoresistance effect associated with magnetic field-induced transformation was clearly observed and the H_0-T curve well accorded with that obtained by previously performed magnetic measurements. The abnormal up-down behavior in the H_0-T curve was clearly reproduced. Electrical resistivity measurements under high magnetic fields showed that the residual electrical resistivity in the P phase at lower temperatures is about $10 \times 10^{-8}\,\Omega$·m, a normal value for the ferromagnetic alloys, whereas the residual electrical resistivity in the M phase is high of about $200 \times 10^{-8}\,\Omega$·m. It was shown that the temperature dependence of the magnetic-field transformation hysteresis can be well described by the Seeger's theory for the plastic deformation at finite temperatures.

Acknowledgements

The authors wish to thank Mr. T. Yasuda and Mr. S. Sasaki at Tohoku Gakuin University for sample preparation. This study was supported by a Grant-in-Aid for Scientific Research from the Japanese Society for the Promotion of Science (JSPS). Part of this work was also supported by a Grant-in-Aid for the High-Tech Research Center Program for private universities from the Japan Ministry of Education, Culture, Sports, Science and Technology.

REFERENCES

1) K. Ullakko, J. K. Huang, C. Kanter, V. V. Kokorin and R. C. O'Handley: Appl. Phys. Lett. **69** (1996) 1966.
2) Y. Sutou, Y. Imano, N. Koeda, T. Omori, R. Kainuma, K. Ishida and K. Oikawa: Appl. Phys. Lett. **85** (2004) 4358.
3) R. Kainuma, W. Ito, Y. Imano, Y. Sutou, H. Morito, S. Okamoto, O. Kitakami, K. Oikawa, A. Fujita, T. Kanomata and K. Ishida: Nature **439** (2006) 957.
4) W. Ito, Y. Imano, R. Kainuma, Y. Sutou, K. Oikawa and K. Ishida: Metall. Mater. Trans. A **38** (2007) 759.
5) T. Krenke, M. Acet, E. Wassermann, X. Moya, L. Mañosa and A. Planes: Phys. Rev. B **73** (2006) 174413.
6) R. Kainuma, Y. Imano, W. Ito, H. Morito, Y. Sutou, K. Oikawa, A. Fujita, K. Ishida, S. Okamoto, O. Kitakami and T. Kanomata: Appl. Phys. Lett. **88** (2006) 192513.
7) S. Y. Yu, L. Ma, G. D. Liu, Z. H. Liu, J. L. Chen, Z. X. Cao, G. H. Wu, B. Zhang and X. X. Zhang: Appl. Phys. Lett. **90** (2007) 242501.
8) V. K. Sharma, M. K. Chattopadhyay, K. H. B. Shaeb, Anil Chouhan and S. B. Roy: Appl. Phys. Lett. **89** (2006) 222509.
9) S. Y. Yu, Z. H. Liu, G. D. Liu, J. L. Chen, Z. X. Cao, G. H. Wu, B. Zhang and X. X. Zhang: Appl. Phys. Lett. **89** (2006) 162503.
10) A. K. Pathak, B. R. Gautam, I. Dubenko, M. Khan, S. Stadler and N. Ali: J. Appl. Phys. **103** (2008) 07F315.
11) B. M. Wang, L. Wang, Y. Liu, B. C. Zhao, Y. Zhao, Y. Yang and H. Zhang: J. Appl. Phys. **106** (2009) 063909.
12) T. Krenke, E. Duman, M. Acet, E. F. Wassermann, X. Moya, L. Mañosa, A. Planes, E. Suard and B. Ouladdiaf: Phys. Rev. B **75** (2007) 104414.
13) T. Krenke, E. Duman, M. Acet, E. F. Wassermann, X. Moya, L. Mañosa and A. Planes: Nature Mater. **4** (2005) 450.
14) V. K. Sharma, M. K. Chattopadhyay and S. B. Roy: J. Phys. D: Appl. Phys. **40** (2007) 1869.
15) Z. D. Han, D. H. Wang, C. L. Zhang, S. L. Tang, B. X. Gu and Y. W. Du: Appl. Phys. Lett. **89** (2006) 182507.
16) B. Zhang, X. X. Zhang, S. Y. Yu, J. L. Chen, Z. X. Cao and G. H. Wu: Appl. Phys. Lett. **91** (2007) 012510.
17) K. Koyama, T. Igarashi, H. Okada, K. Watanabe, T. Kanomata, R. Kainuma, W. Ito, K. Oikawa and K. Ishida: J. Magn. Magn. Mater. **310** (2007) e994.
18) L. S. Sharath Chandra, M. K. Chattopadhyay, V. K. Sharma, S. B. Roy and S. K. Pandey: Phys. Rev. B **81** (2010) 195105.
19) W. Ito, K. Ito, R. Y. Umetsu, R. Kainuma, K. Koyama, K. Watanabe, T. Fujita, K. Oikawa, K. Ishida and T. Kanomata: Appl. Phys. Lett. **92** (2008) 021908.
20) V. K. Sharma, M. K. Chattopadhyay and S. B. Roy: Phys. Rev. B **76** (2007) 140401 (R).
21) K. Kumar, A. K. Pramanik, A. Banerjee, P. Chaddah, S. B. Roy, S. Park, C. L. Zhang and S.-W. Cheong: Phys. Rev. B **73** (2006) 184435.
22) M. A. Manekar, S. Chaudhary, M. K. Chattopadhyay, K. J. Singh, S. B. Roy and P. Chaddah: Phys. Rev. B **64** (2001) 104416.
23) V. V. Khovaylo, T. Kanomata, T. Tanaka, M. Nakashima, Y. Amako, R. Kainuma, R. Y. Umetsu, H. Morito and H. Miki: Phys. Rev. B **80** (2009) 144409.
24) R. Y. Umetsu, W. Ito, K. Ito, K. Koyama, A. Fujita, K. Oikawa, T. Kanomata, R. Kainuma and K. Ishida: Scr. Mater. **60** (2009) 25.
25) R. Y. Umetsu, Y. Kusakari, T. Kanomata, K. Suga, Y. Sawai, K. Kindo, K. Oikawa, R. Kainuma and K. Ishida: J. Phys. D: Appl. Phys. **42** (2009) 075003.
26) R. Zarnetta, *et al.*: Adv. Funct. Mater. **20** (2010) 1917.
27) J. Cui, Y. S. Chu, O. O. Famodu, Y. Furuya, J. Hattrick-Simpers, R. D. James, A. Ludwig, S. Thienhause, M. Wuttig, Z. Zhang and I. Takeuchi: Nat. Mater. **5** (2006) 286.
28) R. Y. Umetsu, A. Fujita, W. Ito, T. Kanomata and R. Kainuma: J. Phys.: Condens. Matter **23** (2011) 326001.

29) X. Xu, W. Ito, R. Y. Umetsu, K. Koyama, R. Kainuma and K. Ishida: Mater. Trans. **51** (2010) 469.
30) X. Xu, W. Ito, M. Tokunaga, R. Y. Umetsu, R. Kainuma and K. Ishida: Mater. Trans. **51** (2010) 1357.
31) A. Seeger: Z. Naturforsch. **9a** (1954) 758.
32) A. Seeger: Z. Naturforsch. **9a** (1954) 856.
33) A. Seeger: Z. Naturforsch. **9a** (1954) 870.
34) A. Seeger: *Dislocations and Mechanical Properties of Crystals*, J. C. Fisher, W. G. Johnston, R. Thomson and T. Vreeland, Jr. (Eds.) New York, (John Wiley, 1957) p. 271.
35) U. F. Kocks, A. S. Argon and M. F. Ashby: *Thermodynamics and Kinetics of Slips*, Progress in Materials Science, ed. by B. Chalmers, J. W. Christian and T. B. Massalski, vol. 19, (Pergamon Press, Oxford, 1975).
36) H. Mecking and U. F. Kocks: Acta Metall. **29** (1981) 1865.
37) G. Ghosh and G. B. Olson: Acta Metall. Mater. **42** (1994) 3371.